NeuroImage 64 (2013) 425–436

Contents lists available at SciVerse ScienceDirect

NeuroImage

journal homepage: www.elsevier.com/locate/ynimg

The neural correlates of velocity processing during the observation of a biological effector in the parietal and premotor cortex

Cinzia Di Dio [a], Giuseppe Di Cesare [a], Satomi Higuchi [c,d,e], Neil Roberts [f], Stefan Vogt [c,d], Giacomo Rizzolatti [a,b,*]

[a] University of Parma, Department of Neuroscience, via Volturno 39/E, 43100 Parma, Italy
[b] IIT (Italian Institute of Technology) Brain Center for Social and Motor Cognition, via Volturno 39, 43100, Parma, Italy
[c] Department of Psychology, Lancaster University, Lancaster LA1 4YF, UK
[d] Magnetic Resonance and Image Analysis Research Centre, University of Liverpool, Pembroke Place, Liverpool, L69 3GE, UK
[e] Center for Experimental Research in Social Sciences, Hokkaido University, N10W7, Kita-ku, Sapporo 060-0810, Japan
[f] Clinical Research Imaging Centre (CRIC), the Queen's Medical Research Institute (QMRI), University of Edinburgh, 47 Little France Crescent, Edinburgh EH16 4TJ, UK

ARTICLE INFO

Article history:
Accepted 4 September 2012
Available online 17 September 2012

Keywords:
Velocity processing
Reaching movements
Biological motion
Dorsal parietal and superior frontal areas
Mirror neurons

ABSTRACT

While there have been several studies investigating the neural correlates of action observation associated with hand grasping movements, comparatively little is known about the neural bases of observation of reaching movements. In two experiments, using functional magnetic resonance imaging (*f*MRI), we defined the cortical areas encoding reaching movements and assessed their sensitivity to *biological motion* and to movement *velocity*. In the first experiment, participants observed video-clips showing either a biological effector (an arm) or a non-biological object (rolling cylinder) reaching toward a target with a biological and a non-biological motion, respectively. In the second experiment, participants observed video-clips showing either a biological effector (an arm) or a non-biological object (an arrow) reaching toward a target with the same biological motion profiles. The results of the two experiments revealed activation of superior parietal and dorsal premotor sites during observation of the *biological motion* only, independent of whether it was performed by a biological effector (reaching arm) or a non-biological object (reaching arrow). These areas were not activated when participants observed the non-biological movement (rolling cylinder). To assess the responsiveness of parietal and frontal sites to movement *velocity*, the *f*MRI repetition–suppression (RS) technique was used, in which movement was shown with same or different velocities between consecutive videos, and observation of identical stimuli was contrasted with observation of different stimuli. Regions of interest were defined in the parietal and frontal cortices, and their response to stimulus repetition was analyzed (same *vs.* different velocities). The results showed an RS effect for velocity only during the observation of movements performed by the *biological effector* and not by the non-biological object. These data indicate that dorsal premotor and superior parietal areas represent a neural substrate involved in the encoding of reaching movements and that their responsiveness to movement velocity of a biological effector could be instrumental to the discrimination of movements performed by others.

Introduction

Accurate perception of movement kinematics is fundamental for understanding the action of another person so as to shape our own behavior accordingly. In the monkey, action observation activates a circuit, which includes, besides visual areas, the superior temporal sulcus region (STS), posterior parietal lobe and premotor cortex. While the STS region is purely visual, both posterior parietal cortex and premotor cortex are endowed with visuo-motor neurons that are active during both the execution and observation of actions (mirror neurons) (Fogassi et al., 2005; Rizzolatti, 2005; Rizzolatti et al., 2001). Transcranial Magnetic Stimulation (rTMS), neurophysiological techniques (EEG, MEG) and brain imaging (PET, *f*MRI) studies have confirmed the existence of the mirror mechanism also in humans (e.g., Buccino et al., 2001; Decety, 1996; di Pellegrino and Wise, 1991; Grafton et al., 1996a, 1996b; Grèzes et al., 2003; Iacoboni et al., 1999; Rizzolatti et al., 1996a, 1996b). Although a number of studies has shown that the mirror mechanism is involved in visuo-motor transformations leading to action understanding (for a review see Rizzolatti and Craighero, 2004; Rizzolatti and Sinigallia, 2010), little is known about how this mechanism responds to the kinematic properties underlying the different types of action.

There is evidence showing that human movements follow kinematic laws describing the geometrical and temporal features of biological

* Corresponding author at: Università degli Studi di Parma, Department of Neuroscience, Via Volturno 39/E, 43100 Parma, Italy. Fax: +39 5021 903900.
E-mail address: giacomo.rizzolatti@unipr.it (G. Rizzolatti).

1053-8119/$ – see front matter © 2012 Elsevier Inc. All rights reserved.
http://dx.doi.org/10.1016/j.neuroimage.2012.09.026

movements. The "two-thirds power law" (Laquaniti et al., 1983), for example, describes a consistent feature of movement execution and, specifically, the relationship between movement trajectory and velocity (Dè Sperati and Viviani, 1997; Hicheur et al., 2005; Viviani and Flash, 1995). In particular, the law links path curvature C and angular velocity A along the movement by a power law with an exponent of 2/3 ($A = KC^{2/3}$, with K as the velocity constant gain factor). As argued in Dayan et al. (2007), this law of motion is a ubiquitous feature of human motor behavior characterizing the kinematic properties of arm movements, smooth pursuit eye movements, speech movements, and movements of the body center of mass during human gait and of the foot during the swing phase of walking.

Behavioral studies suggest that the "two-thirds power law" also influences the perception of other people's movement (Viviani and Stucchi, 1992), and two different *f*MRI studies have shown the neural basis of this effect. Casile et al. (2009) presented subjects with videos in which an animated avatar performed three types of curvilinear arm movements. These movements were either performed with a biological kinematics or with a modified kinematics, created by altering the relationship between tangential velocity and the curvature of the hand trajectories. Dorsal premotor cortex was found to be activated during the observation of movements with biological kinematics, but not during observation of movements performed with modified kinematics. In another *f*MRI study, Dayan et al. (2007) used visual stimuli, which comprised a cloud of points running around an ellipse with different velocities. Relative to the observation of non-biological and constant movements velocity, brain activations increased in the left inferior parietal lobule (IPL) and bilateral dorsal premotor cortex (PMd) when the movements obeyed a biological kinematics. Taken together, these studies suggest that the observation of biological movements obeying the "two-thirds power law" activates the premotor and parietal areas more strongly than the observation of movements not complying with this law.

Previous studies of action observation have mainly investigated hand movements, and particularly grasping movements that involve a hand-object interaction (Binkofski et al., 1999; Buccino et al., 2001; Grafton et al., 1996b; Grèzes et al., 2003). In the present study, we investigated the activation of premotor and parietal areas presenting subjects with video-clips of reaching movements. Specifically, we firstly delineated brain activations during observation of reaching movements following *biological* and *non-biological* motion profiles. Execution and observation of grasping and reaching both produce activation of posterior parietal lobe and premotor areas. In the case of grasping, the action is encoded in ventral parietal and frontal sites (Buccino et al., 2004a, 2004b; Rizzolatti et al., 1996b) whereas, in reaching, we expected action to be encoded in more dorsal parietal and frontal sites (see Filimon et al., 2007).

The second aim of this study was to investigate whether the parietal and frontal sites activated during observation of reaching are sensitive to movement *velocity* and whether responsiveness to velocity in these sites is affected by the *shape* of the moving object (biological *vs.* non-biological). Velocity encoding was studied using the *f*MRI Repetition–Suppression (RS) technique (see Engel and Furmanski, 2001; Fang et al., 2005; Grill-Spector and Malach, 2001; Grill-Spector et al., 1999; Hamilton and Grafton, 2009; Huk et al., 2001; Kourtzi et al., 2005; Lestou et al., 2008; Tolias et al., 2001). In particular, we compared activations when subjects observed either a biological effector or a non-biological object reaching toward a target with the *same* or *different* velocities. The biological effector and the non-biological object moved following the same velocity profiles.

The main results were that, firstly, consistent with previous studies, observation of reaching movements that exhibit a biological kinematics activates parietal and frontal sites located dorsally with respect to the parietal and frontal grasping sites. Secondly, these activations occur independently of whether reaching is performed by a biological effector or a non-biological object, provided that it moves according to a biological kinematics. Thirdly, these sites exhibit a selective responsiveness to velocity when observed reaching is performed by a biological effector, but not by a non-biological object.

Materials and methods

Participants

Fourteen English students (7 females and 7 males, mean age 23.5 years) participated in the first experiment (Exp. 1) that was carried out at the Magnetic Resonance and Image Analysis Research Centre (MARIARC) at the University of Liverpool, UK. Sixteen Italian students (9 females and 7 males, mean age 23.6 years) participated in the second experiment (Exp. 2) that was carried out at the Neuroimaging Centre of the University of Parma, Italy. Subjects were right handed and had normal or corrected-to-normal vision and did not report psychiatric or neurological impairments. They gave fully informed written consent of their willingness to participate. The investigations were approved by the Local Ethics Committees (Liverpool for Exp. 1 and Parma for Exp. 2).

Stimuli

An example of the stimuli used in Exp. 1 is shown in Fig. 1. Specifically, pairs of video-clips were presented to the subjects showing either an arm (Figs. 1A, B) or a cylinder (Figs. 1C, D) moving at different velocities, from a start position to reach a target placed at a distance of 35 cm. The video-clips ended with the arm or the cylinder touching the target. The reaching movements of the arm and of the cylinder were presented at 3 different velocities: low (arm-V1: 0.38 m/s; cylinder-V1: 0.45 m/s), medium (arm-V2: 0.67 m/s; cylinder-V2: 0.78 m/s), and high (arm-V3: 1.5 m/s; cylinder-V3: 1.72 m/s). As a control, a still image of the same arm or of the same cylinder was used, which depicted them in either the start or the end position.

An example of the stimuli used in Exp. 2 is shown in Fig. 2. Specifically, the subjects were presented with video-clips showing either a biological effector (arm, Figs. 2A, B), a non-biological object (arrow — Figs. 2C, D) or a colored biological effector (colored arm — Figs. 2E, F). In contrast to Exp. 1, all stimuli moved according to a biological motion and reaching started from a fixed point (Figs. 2A, C) and ended on a red cross placed at a distance of 46 cm (Figs. 2B, D). The video-clips ended with the arm, the arrow or the colored arm touching the target. The reaching movements of the arm (Arm) and of the arrow (A) were presented at 3 different velocities: low (Arm-V1: 0.35 m/s; A-V1: 0.33 m/s), medium (Arm-V2: 0.89 m/s; A-V2: 0.96 m/s), and high (Arm-V3: 1.83 m/s; A-V3: 1.32 m/s). The 3 colored arms (blue, red, and yellow; Figs. 2E, F) always performed the reaching movement at the same velocity (medium — V2). As a control, a still image of the same arm, arrow or colored arm was used, which depicted them in the end position.

In Exp. 2, the comparison between activations evoked by observation of a biological effector and a non-biological object, both moving following a biological motion, required the construction of an object with a similar shape and moving with similar kinematic profiles as those of the biological effector, i.e. the arm. For this purpose, the arrow was built using a pink-colored stiff paperboard. The tip of the arrow had the same size as the hand (i.e., 15 cm × 11 cm × 4 cm) while the tail of the arrow was the same size as the arm (60 cm × 7 cm × 4 cm) and, therefore, the arrow and the arm occupied the same space in the video-clips. Five hidden wheel-pairs were mounted under the arrow to allow movement. The arrow was pulled from the tip by a transparent nylon thread. Observation of the arrow moving towards the target gave the impression of a reaching movement. Thus, besides controlling for visual and kinematic aspects, the idea of building an arrow was to control for possible high-order effects evoked by the observation of a reaching movement.

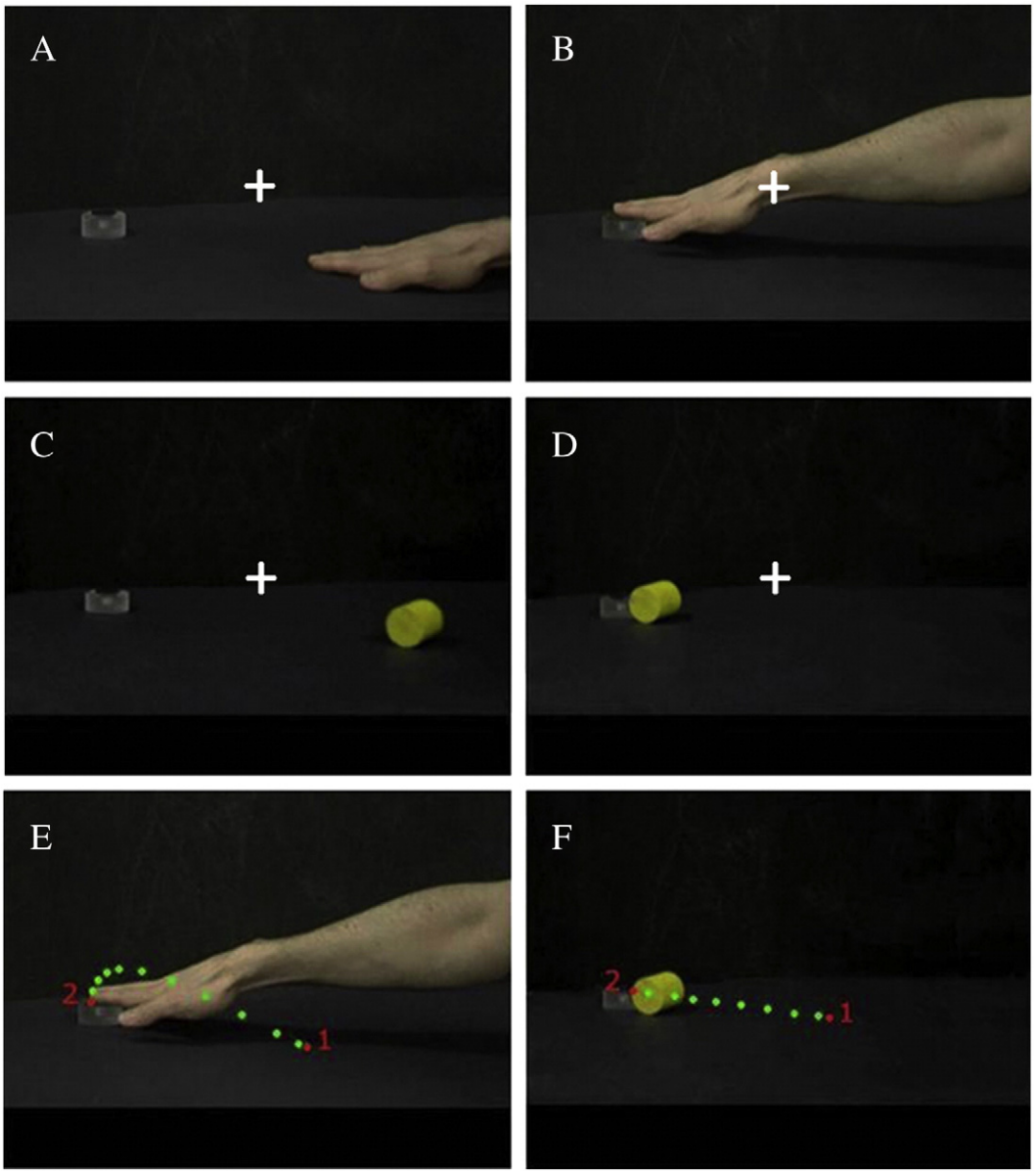

Fig 1. An example of the video-clips as viewed by the participants of Exp. 1. The images show a frame of the arm in the start position (A) and in the end position (B) and of the cylinder in the start position (C) and in the end position (D). The start and the end positions of the arm and of the cylinder were the same. We marked the arm and the cylinder with a green dot on, respectively, the terminal part of the middle finger and of the left border of the cylinder in the start position and marked each occupied position every 40 ms. The arm reached the end point with a translational motion following a curvilinear trajectory E); the cylinder reached the target with a complex motion (rotary + translational) using a straight trajectory (F).

The motion profiles of the arm and arrow were studied using the point kinematics method. Using the software Avimeca v2.3, we marked the positions in the videos of the arm and the arrow with a dot on, respectively, the terminal part of the middle finger of the arm and the inferior vertex of the arrow tip in the start position (Figs. 3A, C) and marked each occupied position in space every 40 ms. In this way, we were able to verify that the arm and the arrow moved with equivalent trajectory and occupied the same positions in time.

By using Regressi software (version 2.9) we obtained velocity curves for both stimuli (Figs. 3B, D). To make sure that velocity varied in the same fashion in the two stimuli (arm and arrow) and within each velocity level (V1, V2, V3), we carried out a 2×3 repeated measures GLM analysis. For homogeneity of comparison between stimuli and across velocity levels, we considered only a number of values ranging ±6 around the pick of each velocity/type level, totaling 13 values (corresponding to the minimum amount of recorded values associated with V1).

Independently of velocity level (V1, V2, V3), the results showed no significant differences in mean velocity between stimuli ($P>.05$), indicating that the two stimuli had a similar velocity profile. Additionally, data showed a main effect of velocity ($F_{2,24}=11.87$; $P<.001$; partial-$\eta^2=.50$; $\delta=.99$) and no interaction effects between stimulus-type and velocity ($P>.05$). Simple contrast analyses between the 3 velocity levels across stimulus-type showed a significant difference between V1 and V2 ($F_{1,12}=53.59$; $P<.001$; partial-$\eta^2=.82$; $\delta=1$) and between V2 and V3 ($F_{2,24}=11.87$; $P<.05$; partial-$\eta^2=.37$; $\delta=.68$). These results confirmed similar velocity patterns for the arm and the arrow as well as differences across velocity levels for both stimuli.

Paradigm and task

To assess brain responses to observed movement velocity, the RS technique was used in both Exp. 1 and Exp. 2. In Exp. 1, pairs of video-clips

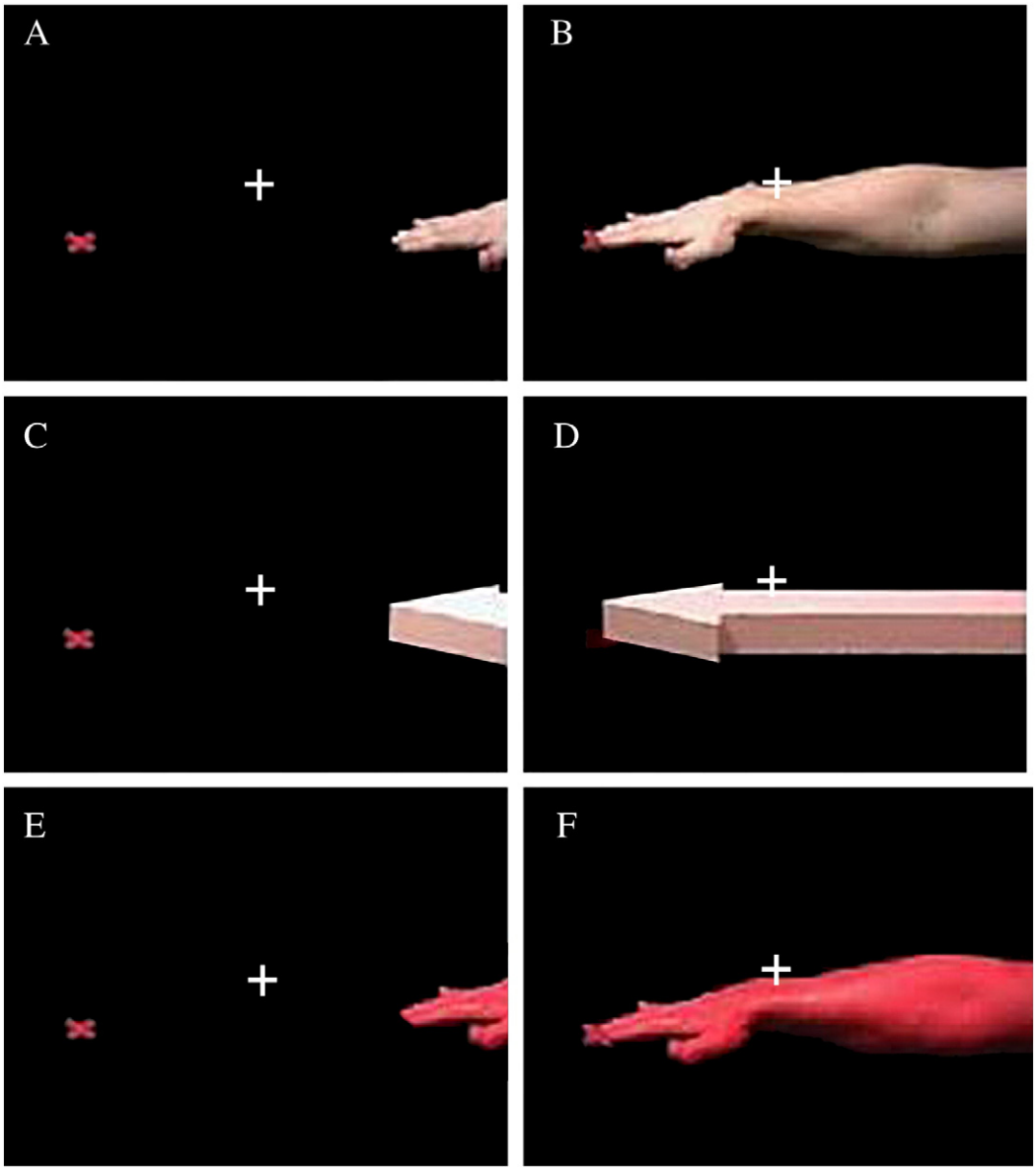

Fig. 2. An example of the video-clips as viewed by the participants of Exp. 2. The arm, the arrow and the colored arm are shown at the start position (A, C, E) and at the end position marked by a red cross (B, D, F). In the conditions *same*, the arm and the arrow reached the end point with the same velocity between video-pairs and, in the conditions *different*, with different velocities between video-pairs. The colored arm reached the end point always at the same velocity but changing, in the conditions *different*, the color of the arm between video-pairs.

presented consecutively either the arm or the cylinder moving with the same velocity (condition *same*: 48 trials) or with different velocities (condition *different*: 48 trials). In Exp. 2, pairs of video-clips showed the arm, the arrow or the colored arm moving with the same velocity/color between consecutive videos (condition *same*: 30 trials) or with different velocities/color (condition *different*: 30 trials). The trials were constructed so that all possible order combinations of velocity (condition *same*: V1–V1; V2–V2; V3–V3; condition *different*: V1–V2; V1–V3; V2–V3; V3–V1; V3–V2) and of color-C (condition *same*: C1–C1; C2–C2; C3–C3; condition *different*: C1–C2; C1–C3; C2–C3; C3–C1; C3–C2) were presented.

Each scanning session (functional run) started with a cross positioned at the centre of the screen (500 ms) on which subjects were instructed to fixate and that remained on the screen throughout the trials. The first video-clip was presented for 2 s followed by a 100 ms interval before the second video-clip, which was presented for 2 s. The second video was followed by a jittered interval ranging between 2 and 7 s. In about 17% of cases in Exp. 1 and 29% of cases in Exp. 2, subjects were asked to provide an explicit response to the stimuli during this interval (catch trials).

During the catch trials, cued by the appearance of a question mark after the second video offset, the subjects had to indicate, on a response box, whether the two consecutive videos were the same or different. About 20% of the trials were characterized by two consecutive videos representing a still image of the arm, the cylinder, the arrow or the colored arm (control still image).

In Exp. 1, the subjects viewed a total of 342 trials comprising video-pairs distributed among conditions as follows: 96 trials of arm movement (no overt response) plus 18 catch trials (with response); 96 trials of object movement (no overt response) plus 18 catch trials (with response); 32 trials of static arm (no overt response) plus 6 catch trials (with response); 32 trials of static object (no overt response) plus 6 catch trials (with response). In Exp. 2, subjects viewed a total of 315 trials comprising video-pairs distributed among conditions as follows: 60 arm reaching (Arm; 30 same, 30 different), 60

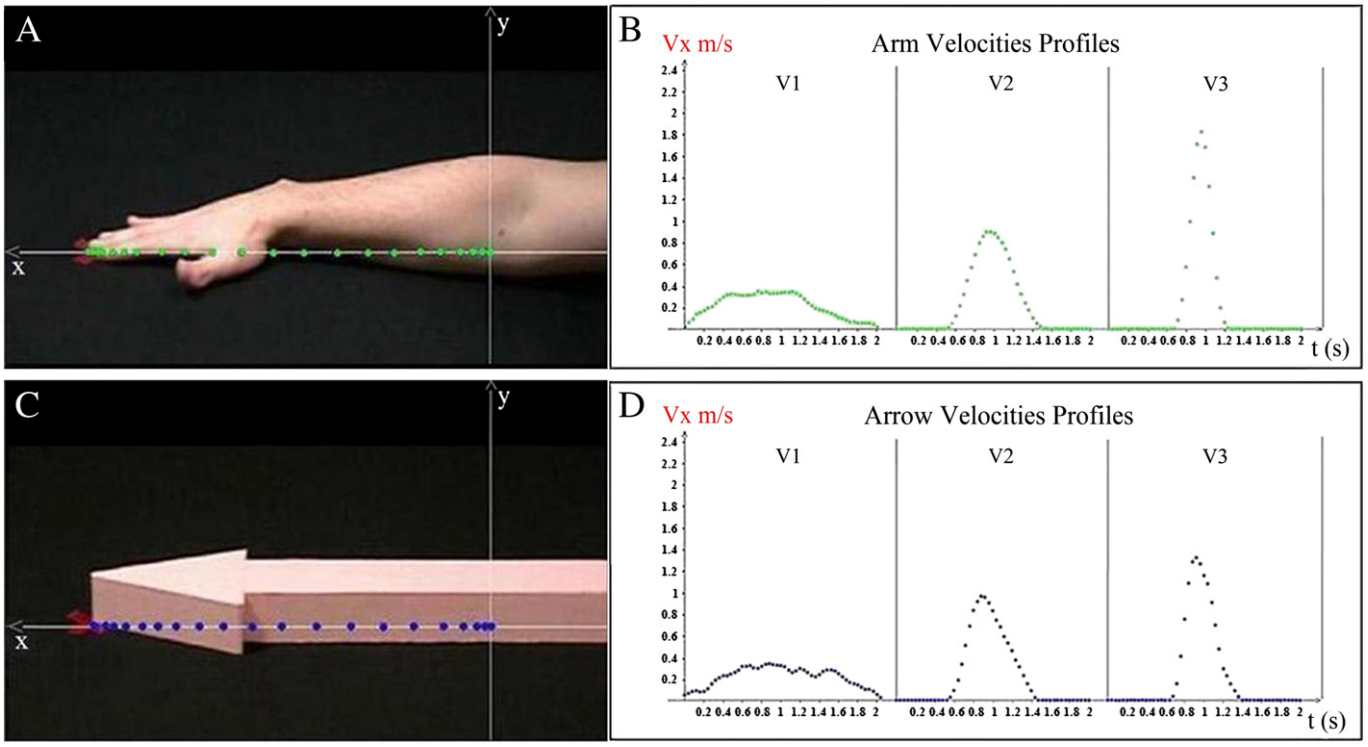

Fig. 3. Trajectory profile of the arm (A) and of the arrow (C) reaching the end point with a biological motion. X and Y spatial coordinates are shown in the figure with colored dots that indicate the values of each point occupied in space and time by the arm and arrow moving with a medium velocity (V2). Graphs showing velocity profiles for the arm (B) and for the arrow (D) reaching movements at low velocity (V1 mean peak for the arm: 0.35 m/s at 0.75 s; V1 mean peak for the arrow: 0.33 m/s at 0.88 s); medium velocity (V2 mean peak for the arm: 0.89 m/s at 0.91 s; V2 mean peak for the arrow: 0.96 m/s at 0.88 s) and high velocity (V3 mean peak for the arm: 1.83 m/s at 0.96 s; V3 mean peak for the arrow: 1.32 m/s at 0.91 s). (For interpretation of the references to color in this figure legend, the reader is referred to the web version of this article.)

arrow reaching (A; 30 same, 30 different), 60 colored arm reaching (CArm; 30 same, 30 different), 15 still arm, 15 still arrow, 15 colored arm (still) and 90 catch trials. The experiments lasted approximately 60 min divided in 4 functional runs in Exp. 1 and 5 functional runs in Exp. 2, with each run lasting about 11 min. Stimuli were randomized within each run and balanced across runs so that there was an equal number of trials of each condition type.

In Exp. 1, the stimuli were viewed through a frontal mirror mounted on the head coil of the MR system to reflect images displayed on a screen via a projector positioned outside the scanner room. Presentation 11.0 (Neurobehavioral Systems, Albany, CA, http://www.neurobs.com) was used for stimulus presentation and response recording. In Exp. 2, the stimuli were viewed via digital visors (VisuaSTIM) with a resolution of 500,000 pixels per 0.25 square inch and horizontal eye field of 30°. The digital transmission of the signal to the scanner was via optic fiber. E-Prime 2 Professional software (Psychology Software Tools, Inc., Pittsburgh, USA, http://www.pstnet.com) was used for stimulus-presentation and recording of the subjects' answers.

A training session was given prior to scanning to familiarize subjects with the experimental procedure.

Image acquisition

In Exp. 1, *f*MRI data were acquired on a 3 T Trio whole-body scanner with eight-channel head coil (Siemens Medical System, Erlangen, Germany). Echo-planar images (EPIs) were obtained using a gradient-echo sequence with the following parameters: echo time TE = 30 ms, repetition time TR = 2000 ms, flip angle = 90°, field of view FoV = 192 × 192 mm^2, slice thickness = 3 mm, inter-slice gap = 1.2 mm, in-plane resolution = 3 × 3 × 4.2 mm^3, Bandwidth = 2604 Hz/Px, Echo spacing = 0.45 ms. The FoV was tilted by 30° in a clockwise direction to encompass the whole brain with 32 interleaved transverse slices. Each of the 4 functional runs comprised 333 sequential volumes. A T1 weighted structural image was also obtained with the following parameters: TE = 5.57 ms, TR = 2040 ms, flip angle = 8°, FoV = 224 × 256 mm^2, slice thickness = 1 mm, in-plane resolution = 1 × 1 × 1 mm^3, SENSE factor = 2. Total scanning time was approximately 60 min.

In Exp. 2, *f*MRI data were acquired with a 3 T SIGNA whole-body scanner with eight-channel head coil (General Electrics, Milwaukee, USA). Echo-planar images (EPIs) were obtained using a gradient-echo sequence with the following parameters: echo time TE = 30 ms, repetition time TR = 2100 ms, flip angle = 90°, field of view FoV = 192 × 192 mm^2, slice thickness = 3 mm, inter-slice gap = 0.5 mm, in-plane resolution = 2.5 × 2.5 × 2.5 mm^3, Bandwidth = 3906 Hz/Px, Echo spacing = 0.44 ms. The FoV was tilted 30° in a clockwise direction to encompass the whole brain with 37 interleaved transverse slices. Each of the 5 functional runs comprised 310 sequential volumes. A T1 weighted structural image was obtained with the following parameters: TE = 3.2 ms, TR = 8200 ms, flip angle = 12°, FoV = 256 × 256 mm^2, slice thickness = 1 mm, in-plane resolution = 1 × 1 × 1 mm^3, acceleration factor arc = 2. Total scanning time was approximately 60 min.

Statistical analysis

Data analysis was performed using SPM8 (Statistical Parametric Mapping software; The Wellcome Department of Imaging Neuroscience, London, UK; http://www.fil.ion.ucl.ac.uk) running in MATLAB R2009b (The Mathworks, Inc., Natick, MA). The first four EPI volumes of each functional run were discarded to allow for T1 equilibration effects. For each subject, all volumes were spatially realigned to the first volume of the first functional run and un-warped to correct for between-scan motion. The T1 weighted image was segmented into gray, white and cerebrospinal fluid and spatially normalized to the Montreal Neurological Institute (MNI) space. The spatial transformation derived from this segmentation was then applied to the realigned EPIs

for normalization and re-sampled in $2\times2\times2$ mm^3 voxels using trilinear interpolation in space. All functional volumes were then spatially smoothed with a 6 mm full-width half-maximum isotropic Gaussian kernel for the group analysis.

Data were analyzed using a random-effects model (Friston et al., 1999), implemented in a two-level procedure. In the first level, single-subject *f*MRI responses were modeled using a General Linear Model (GLM), for which a design-matrix included the onsets and durations of each event for each stimulus-type (Exp. 1: Arm, C; Exp. 2: Arm, A, CArm) and condition (*same*, *different*) for each functional run. In Exp. 1, eight regressors were modeled (Armsame, Armdiff, Armstill, Csame, Cdiff, Cstill, CatchTrials and Response). In Exp. 2, eleven regressors were modeled (Armsame, Armdiff, Armstill, Asame, Adiff, Astill, CArmsame, CArmdiff, CArmstill, CatchTrials and Response). In both Exp. 1 and Exp. 2, all regressors, except for Response, included the two consecutive videos of each trial, which were modeled as one single epoch lasting 4.1 s. Responses were modeled as event-related.

In the second level analysis (group-analysis), corresponding contrast images of the first level for each subject were entered in two flexible ANOVAs with sphericity-correction for repeated measures (Friston et al., 2002). The first model considered the pattern of activation of the 2 stimulus-types (Arm, C; Exp. 1) and the 3 stimulus-types (Arm, A, CArm; Exp. 2), pooling together the two conditions *same* and *different* minus each respective still image (control still image). This model was used for localization of regions of interest (ROIs, see next section). The second model was created considering the 2 stimulus-types (Arm, C; Exp. 1) and the 3 stimulus-types (Arm, A, CArm; Exp. 2) for each condition (*same* and *different*) separately minus each respective still image (Armstill, Cstill, Astill and CArmstill). This model was used for signal change extraction at the subject level, as specified in the ROI analysis below.

Results were thresholded at $P<0.05$ family wise error (FWE) corrected at the cluster or voxel level as appropriate (cluster size estimated with a voxel-level threshold of *P*-uncorrected = 0.001). The location of foci of activation is presented in the stereotaxic space of the MNI coordinate system. Activations were also localized with reference to cytoarchitectonical probabilistic maps of the human brain, using the SPM-Anatomy toolbox v1.7 (Eickhoff et al., 2005).

Repetition–suppression and ROI analysis

The RS analysis (Grill-Spector et al., 1999; Hamilton and Grafton, 2009; Kourtzi et al., 2005; Lestou et al., 2008) was used to assess the neural response to observed velocity during observation of the reaching movements. Within the RS analysis, activations obtained when the subjects were presented with pairs of videos showing the same stimulus (condition *same*) were compared with those associated with observation of pairs of videos differing in one specific dimension (condition *different*). In Exp. 1, differences for both the arm and the cylinder were analyzed with respect to movement velocity (low — V1; medium — V2; high — V3). In Exp. 2, for the arm and the arrow, differences were analyzed with respect to movement velocity as in Exp. 1; for the colored arm, differences were analyzed with respect to the arm color (red — C1, yellow — C2, blue — C3).

To test the RS effect of movement velocity within the cortical sites active during reaching observation, ROIs were defined on the basis of the functional maps obtained from the second-level group analysis (see statistical model 1 above). More specifically, ROIs were defined within the functional maps reflecting global activations within the parietal and frontal sites in response to at least one of the regressors of interest, namely: only the arm (— still) in Exp. 1 (since the cylinder produced no activation in this sites); the arm, the arrow, and the colored arm (— still) in Exp. 2, independently of conditions *same* and *different* ($P_{FWE\text{-}corr}<.05$ at the voxel level). In total, two ROIs were defined reflecting the cluster of activation in left dorsal premotor (PMd) and left superior parietal lobule (SPL), respectively.

The mean cluster values were calculated for each ROI and stimulus-type (Exp. 1: Arm, C; Exp. 2: Arm, A, CArm) separately for the two conditions (*same* and *different*) *vs.* control still images — see statistical model 2 above. Signal change for each subject was extracted using REX (http://web.mit.edu/swg/rex). One subject of Exp. 2 was excluded from the analysis as an extreme case.

Results

Experiment 1

Overall effect of reaching observation

The brain activations obtained by comparing arm reaching (independently of the conditions *same* or *different*) *vs.* the control still images of the same arm are shown in Fig. 4A. Activations were found in occipital lobe, including V6, bilateral human putative MT/V5 complex, left intraparietal sulcus, straddling the inferior and superior banks, left ventral and dorsal premotor cortex and deep structures, including right insula (see Table 1a for coordinates and statistical values).

The contrast between observation of the rolling cylinder and observation of the control still images of the same cylinder, independently of conditions (*same* or *different*), produced activations in bilateral human putative MT/V5 complex (Fig. 4B, Table 1b).

Repetition–suppression effect

Within the RS analysis, we compared activations observed when subjects were presented with pairs of videos showing the arm or the cylinder moving at the same velocity (condition *same*) or at different velocities (condition *different*) between videos. The RS analysis was performed for 2 ROIs: one in left dorsal premotor cortex (PMd) and one in left superior parietal lobule (SPL), i.e. in the parietal and frontal regions activated during observation of the arm reaching movement. The difference between the conditions *different* and *same* (RS effect) for the arm and the cylinder were tested in a 2×2 repeated measures GLM analysis, with 2 levels of stimulus-type (Arm, C) and 2 levels of stimulus-condition (*same*, *different*) independently for each PMd and SPL ROIs.

With respect to the activations observed for the PMd ROI, results revealed a main effect of stimulus-type (Arm > C; $F_{1,12}=12.8$, $P=.004$, partial-$\eta^2=.52$, $\delta=.91$) and a significant interaction stimulus-type × condition ($F_{1,12}=14.6$, $P=.002$, partial-$\eta^2=.55$, $\delta=.94$). Similarly, results for the SPL ROI revealed a main effect of stimulus type (Arm > C; $F_{1,12}=9.33$, $P=.01$, partial-$\eta^2=.44$, $\delta=.8$) and a significant interaction stimulus-type × condition ($F_{1,12}=5.3$, $P=.04$, partial-$\eta^2=.31$, $\delta=.56$).

As shown in Figs. 4C, D, independent post-hoc analyses for PMd and SPL revealed a significant difference between conditions *same* and *different* (*different* > *same*) for the arm only (PMd: $F_{1,12}=4.7$, $P<.05$, partial-$\eta^2=.28$, $\delta=.52$; SPL: $F_{1,12}=5.4$, $P<.05$, partial-$\eta^2=.31$, $\delta=.57$).

Experiment 2

In Exp. 2, subjects observed two types of moving stimuli: a biological one, i.e. an arm, and a non-biological one, i.e. an arrow. Both stimuli moved with three different velocities (see Fig. 3 and Methods section for details). A third stimulus, i.e. a reaching arm whose color — instead of velocity — changed in the conditions *different*, was also introduced to rule out possible attention-related effects on the observed activations (see Bartels et al., 2008).

Overall effect of reaching observation

Arm vs. control still image. The brain activations obtained by comparing observation of the arm reaching movement, pooling together the conditions *same* and *different*, *vs.* the control still images of the

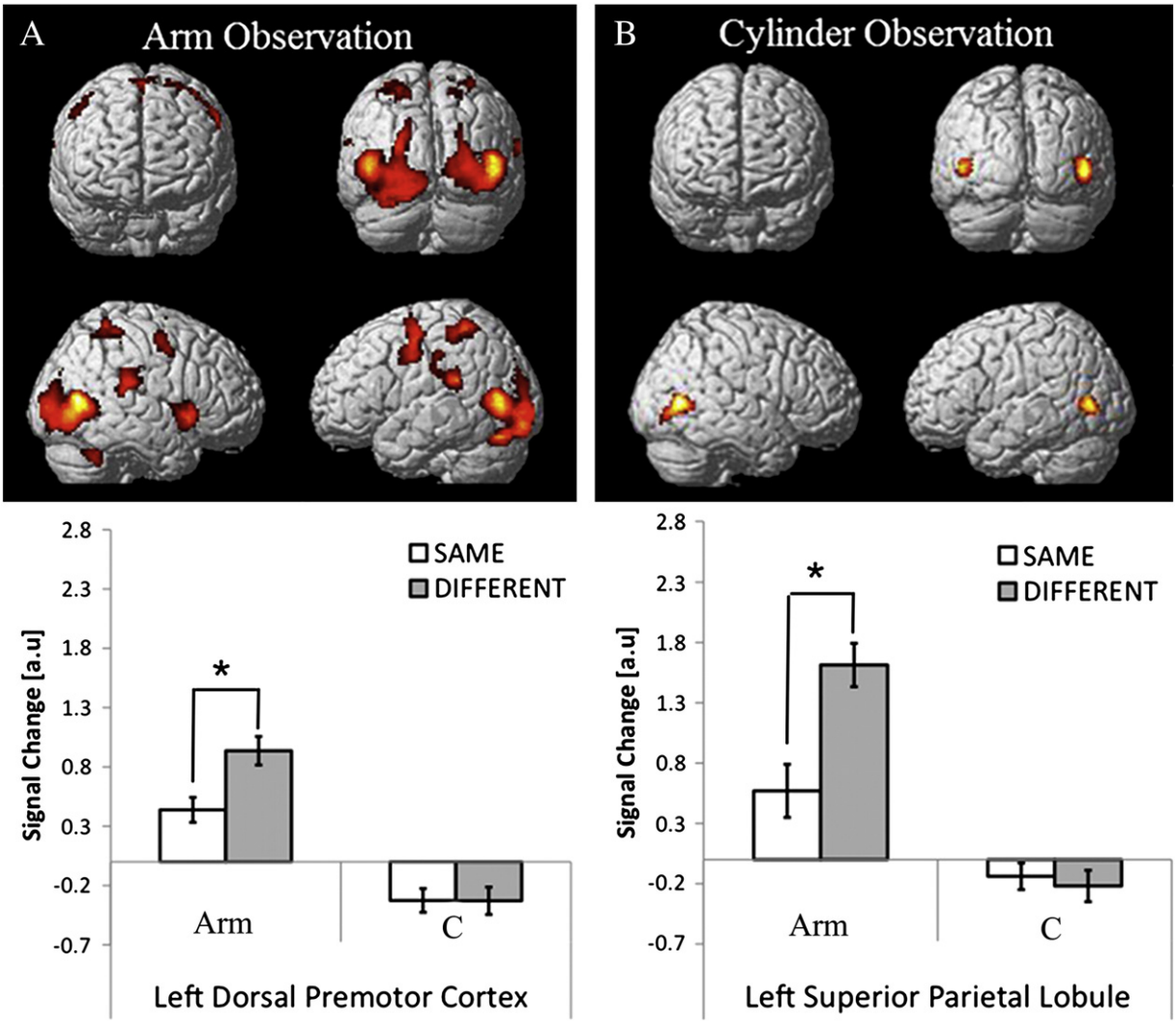

Fig. 4. Cerebral activities in Exp. 1 during the observation of the arm reaching movement (A) and of the rolling cylinder (B), pooling together the conditions *same* and *different*, *vs.* control still images (still images of each respective stimulus-type). The statistical parametric maps (group average) are mapped onto a standard MNI ($P_{FWE\text{-}corr}<.05$). The graphs display the mean signal change in arbitrary units (a.u.) in the conditions *same* (white bars) and *different* (gray bars) for each stimulus-type (Arm — Arm, cylinder — C) within (C) the dorsal premotor cortex (PMd; maxima: −22 −8 60) and (D) superior parietal lobule (PLd; maxima −28 −46 56). The error bars represent the standard error of the mean. Asterisk (*) indicates significant differences between the conditions *different–same* ($P<.025$). (For interpretation of the references to color in this figure legend, the reader is referred to the web version of this article.)

same arm are shown in Fig. 5A. Activations were observed in left superior occipital lobe, including area V6, bilateral human putative MT/V5 complex, left superior parietal lobule (SPL) extending into the intraparietal sulcus and left dorsal premotor cortex (PMd), right prefrontal cortex and bilateral insula (see Table 2a, Arm, for coordinates and statistical values).

Arrow vs. control still image. Observation of the non-biological object (arrow — A) performing a reaching movement towards a point with *biological motion*, independently of conditions *same* or *different*, produced signal increase, with respect to the control still images of the same arrow, in areas encoding reaching movement. As shown in Fig. 5B, the main areas activated involve left superior occipital lobe, including area V6, bilateral human putative MT/V5 complex, an area straddling the superior temporal gyrus and inferior parietal lobule (area TPJ), left superior parietal lobule (SPL) extending into intraparietal sulcus, bilateral dorsal premotor cortex (PMd) and bilateral insula (see Table 2a, Arrow, for coordinates and statistical values).

The interaction between observation of the arm and the arrow reaching movements, relative to their respective static controls, showed no activation for the arm *vs.* the arrow as well as for the opposite contrast.

Colored Arm vs. control still image. As shown in Fig. 5C, observation of the reaching movement of the colored arm (independently of the conditions *same* or *different* color) revealed enhanced activations, with respect to the control still images of the same colored arm, in left superior occipital lobe including area V6, bilateral human putative MT/V5 complex, left superior parietal lobule and left dorsal premotor cortex (see Table 2a, CArm, for coordinates and statistical values).

Repetition–suppression effect

For the RS analysis, we first carried out a global activation analysis across the three stimulus-types (arm, arrow, colored arm), independently of the conditions *same* and *different, vs.* each respective control still images ($P_{FWE\text{-}COR\text{-}VXL}<.05$). As shown in Fig. 6A, global activations were observed in left superior occipital lobe including area V6, human putative MT/V5 complex, superior parietal lobule (mostly on the left side) and bilateral dorsal premotor cortex (see Table 2b for coordinates and statistical values).

Table 1
a. Activations in Exp. 1 during the observation of the Arm *vs.* control still images; b. activations during the observation of the Cylinder *vs.* control still images. Local maxima of activated areas, as shown in Fig. 4, are given in MNI standard brain coordinates at cluster-level $P<.05$ and voxel level $P<.001$ [ATB: most probable anatomical region in the Anatomy Toolbox 1.7, Eickhoff et al., 2005; asterisks (*) denote assigned areas].

Anatomical region	Left					Right				
	x	*y*	*z*	*Z*-score	ATB	*x*	*y*	*z*	*Z*-score	ATB
Stim-type vs. control still image ($P_{UNCOR\text{-}VXL}=<.001$)										
a. Arm (Arm)										
Superior occipital gyrus/V6	−20	−80	28	4.49		22	−80	28	3.54	
Lingual gyrus	−18	−86	−2	5.65	30% hOC3V (V3v)*					
Middle occipital gyrus/V5	−40	−70	8	5.87	30% hOC5 (V5)	48	−76	0	5.33	20% hOC5 (V5)
Superior temporal gyrus	−44	−42	12	4.92						
Middle temporal gyrus/V5						48	−70	12	6.73	
Superior parietal lobule (SPL)	−28	−46	56	5.76	40% Area 2*	22	−50	54	4.70	60% SPL (7PC)*
IPS	−42	−28	40	4.33	40% IPC (Pft)*					
Superior marginal gyrus	−48	−28	28							
Rolandic operculum						60	−28	24	4.27	40% OP1*
Postcentral gyrus (PMd)	−22	−8	60	4.50	30% Area 6	42	−4	54	4.25	40% Area 6
Postcentral gyrus (PMv)	−52	−6	40	5.14	60% Area 6					
Insula						38	8	2	4.49	
Cerebellum	−28	−72	−20	5.48	51% Lobule VI*					
b. Cylinder (C)										
Middle occipital gyrus	−40	−70	6	4.76	20% hOC5 (V5)	48	−78	2	4	20% hOC5 (V5)
Middle temporal gyrus/V5						46	−68	8	4.91	30% hOC5 (V5)

Given the lack of activation of right parietal and frontal sites for the arm and colored arm and of right parietal cortex for the arrow reaching movements (with respect to each respective control still images — see analyses above), two ROIs were defined centering on the activations observed in left premotor and parietal cortices (see Methods). The RS effect for velocity and color were then tested in these ROIs.

Within the RS analysis, we compared activations observed when participants were presented with pairs of videos showing the same stimulus (condition *same*) and pairs of videos differing in one specific dimension (condition *different*) between videos. For the arm and the arrow, differences were analyzed with respect to movement velocity (low — V1; medium — V2; high — V3); for the colored arm differences were analyzed with respect to the arm color (red, yellow, blue).

Comparisons between conditions *different* and *same* (RS effect) among the 3 stimulus-types (Arm, A, CArm) were tested in 3×2 repeated measures GLM analysis, with 3 levels of stimulus-type and 2 levels of stimulus-condition (*same*, *different*) independently for each ROI. Interaction effects were tested post-hoc and adjusting the *P*-values according to the Bonferroni correction for multiple comparisons ($P=.05/3=.017$). Descriptive analyses and the statistical values relative to the direct comparison between conditions *same* and *different* for each stimulus-type are summarized in Table 3.

As shown in Fig. 6B, C, results for both PMd and SPL showed a main effect of stimulus-condition (*different*>*same*; PMd: $F_{1,14}=15.73$, $P<0.05$, partial-$\eta^2=.53$, $\delta=.96$; SPL: $F_{1,14}=7.96$, $P<.05$, partial-$\eta^2=.36$, $\delta=.75$) as well as a significant interaction for stimulus-type× stimulus-condition (PMd: $F_{2,28}=4.34$, $P<.05$, partial-$\eta^2=.24$, $\delta=.49$; SPL: $F_{2,28}=3.63$, $P<.05$, partial-$\eta^2=.21$, $\delta=.62$).

For both PMd and SPL, post-hoc analyses revealed a significant difference between conditions *same* and *different* for arm reaching observation only (PMd: $F_{1,14}=30.5$, $P<.0001$, partial-$\eta^2=.69$, $\delta=.99$; SPL: $F_{1,14}=10.9$, $P=.005$, partial-$\eta^2=.44$, $\delta=.87$). No differences were observed for either the arrow or the colored arm ($P>.05$; see Table 2 for descriptive statistics).

Discussion

The aim of the present study was to delineate the cortical regions that are specifically involved in processing the observation of reaching movements and to investigate their sensitivity to *biological motion*. Additionally, using the RS technique (RS; Grill-Spector et al., 1999; Hamilton and Grafton, 2009; Kourtzi et al., 2005; Lestou et al., 2008) we investigated the responsiveness of these regions to the observation of reaching movements performed with different *velocities*. Two experiments were carried out. In Exp. 1, video-clips showed either an arm (biological effector) or a cylinder (non-biological object) reaching toward the same target with biological and non-biological motions, respectively. In Exp. 2, the video-clips showed an arm (biological effector) or an arrow (non-biological object) reaching toward a target following the same biological motion.

The results of Exp. 1 showed activations specific to the arm reaching movements *vs.* control still images of the same arm in visual occipito-temporal areas, including MT/V5 and V6, in intraparietal sulcus, straddling the inferior and superior banks, and ventral and dorsal premotor cortex. All activations were bilateral, although stronger in the left hemisphere. The analysis contrasting the rolling movements of the cylinder *vs.* control still images of the same cylinder showed enhanced activations in bilateral MT/V5 complex. The lack of activation of the parietal and frontal sites in response to observation of the rolling cylinder confirms previous studies (e.g., Casile et al., 2009; Dayan et al., 2007) showing that these areas do not respond to non-biological movements.

The results of Exp. 2, where we compared separately activations observed for the arm and the arrow reaching movements *vs.* their respective control still images, revealed, for both stimulus-types, activations of visual and temporal areas, including MT/V5 and V6, left superior parietal lobule and left dorsal premotor cortex.

Activation of the parietal and frontal areas during observation of reaching movements is consistent with previous findings showing their involvement in both reaching execution and observation (Filimon et al., 2007). Both our data and Filimon and colleagues' study indicate that activations associated with reaching are located more dorsally than those described for grasping. A large number of investigations, in fact, shows that grasping is encoded in the human AIP and the adjacent inferior parietal lobule, as well as in the frontal lobe, mostly in the ventral premotor cortex extending into the posterior part of the inferior frontal gyrus (Buccino et al., 2001; Culham, 2004; Grafton et al., 1996b; Grèzes et al., 2003; Rizzolatti et al., 1996a, 1996b).

A significant new finding of the present study is the overlap between the motor activations elicited by the observation of the arm reaching movements and those elicited by the observation of the reaching arrow. These regions were not activated during the observation of the non-biological movement (rolling cylinder), suggesting that the dorsal parietal and superior frontal sites respond to *biological motion* only,

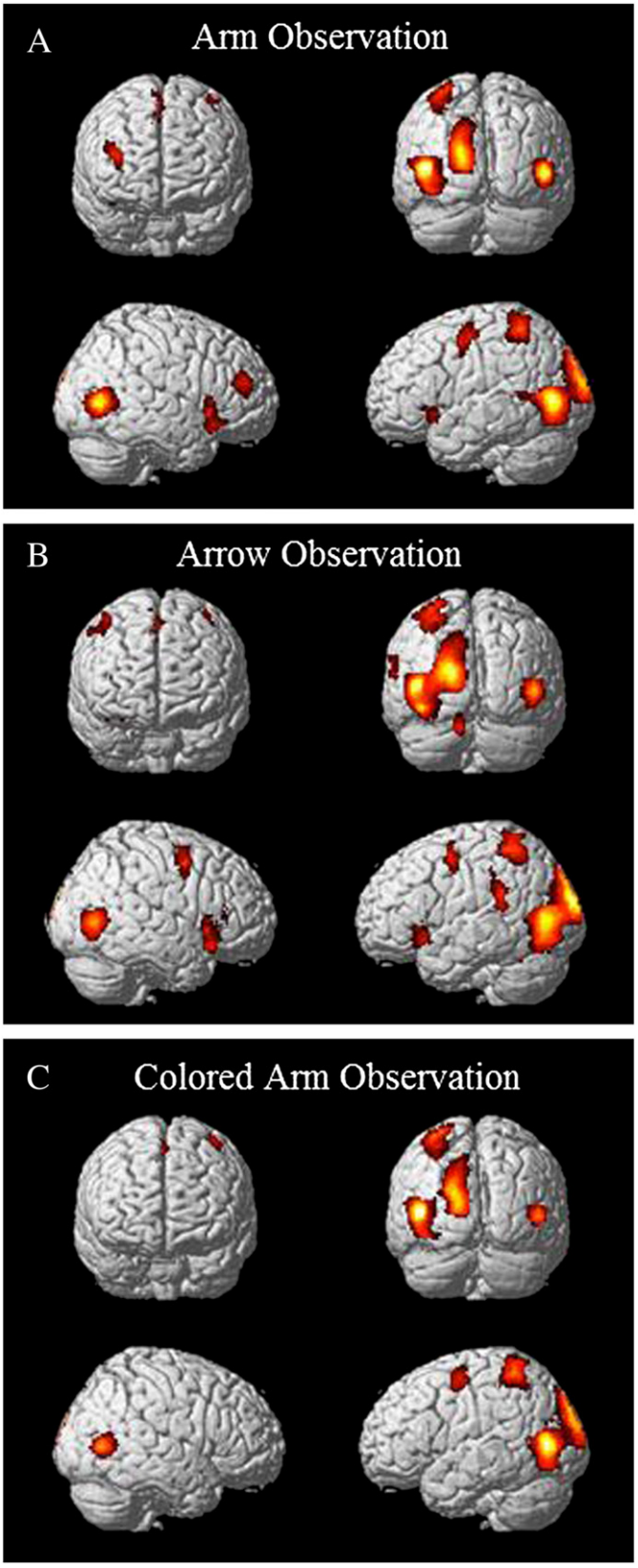

Fig. 5. Cerebral activities in Exp. 2 during observation of the arm (A), the arrow (B) and the colored arm (C) reaching movements, pooling together the conditions *same* and *different*, *vs.* control still image (still images of each respective stimulus-type). The statistical parametric maps (group average) are mapped onto a standard MNI ($P_{FWE\text{-}corr} \leq .05$).

independently of the shape of the moving stimulus (biological or non-biological).

Comparison of the parietal and premotor activations in response to the arm reaching movement between Exp. 1 and Exp. 2 revealed that the activations in Exp. 1 extended further ventrally than those observed in Exp. 2. A possible explanation for this divergence might be the different targets used in the two experiments. Although the video-clips in Exp. 1 always presented a reaching arm purely touching the object, because the reaching-target was a graspable 3-D object this could have triggered in the observers a motor program for grasping (Gibson, 1986; Grafton et al., 1996b; Grèzes et al., 2003; Rizzolatti et al., 1996a, 1996b). In contrast, in Exp. 2, the target-object was a 2-D cross that did not afford any grasping action. This marker primed a grasp-independent reaching movement eliciting activation selectively in the dorsal parietal and superior frontal sites.

In order to investigate sensitivity of the parietal and frontal sites to movement *velocity* using the *f*MRI RS technique, two ROIs were defined for use in both Exp. 1 and Exp. 2. One ROI was defined in left dorsal premotor cortex (PMd) and one in left superior parietal lobule (SPL) that were strongly activated during observation of the biological movements. The RS effect within these regions was tested by contrasting the conditions in which video-pairs presented consecutive stimuli moving with different velocities between videos (condition *different*) with those in which velocity remained unchanged (condition *same*). The RS results revealed, in both premotor and parietal ROIs, a suppression effect only for the arm reaching velocity and not for the arrow, showing that activation of the dorsal parietal and frontal sites is modulated by *velocity* only during observation of movements performed by a *biological effector* (i.e., the arm).

Altogether, the results of the present study suggest that the dorsal parietal and frontal sites specifically encode biological motion (Exp.1) and generalize across different shapes (Exp. 2), whereas these sites only encode velocity when a biological effector is involved (Exp. 2). What possible neural mechanisms may then account for the activation pattern observed in this study?

Although it is not possible to specify the precise neural mechanisms here involved, some hypotheses can be advanced on the basis of previous *f*MRI studies as well as from neuroanatomical experiments with non-human primates. In monkeys, the accepted view is that visual information of the dorsal visual stream terminates in IPL and SPL. The classical view on the organization of the dorsal stream was that its nodal area is MT/V5. This area receives direct input from the striate visual area V1 and from other extrastriate visual areas. *f*MRI experiments in humans confirmed the role of MT/V5 as a fundamental node in movement processing (e.g., Sunaert et al., 1999; Zeki et al., 1991).

It has been subsequently discovered that visual information travelling the dorsal stream has another nodal area, i.e. area PO (Colby et al., 1988), that has been subdivided into two different areas: the occipital area V6 and the parietal area V6A. In the monkey, V6 is located within the posterior occipital sulcus (POS) and borders with V6A that occupies the dorsal sector of the same bank. While V6 is a purely visual area, receiving input from the striate and extrastriate visual areas, V6A belongs to the parietal lobe and is endowed with more complex properties. In humans, recent *f*MRI studies have shown that the putative V6 complex is located in the occipito-parietal junction (Pitzalis et al., 2009) and it is likely that this complex contains visual and somatic neurons involved in the control of reach-to-grasp movements.

One possible explanation for SPL response to movement velocity of the biological effector rests on recent *f*MRI findings with humans showing MT preferred activation for biological movements (hand actions) than non-biological movements (Jastorff et al., 2010). Since MT/V5 is connected to area V6, it is possible to hypothesize that visual information about movement of the biological shape reaches SPL through this pathway (see also Galletti et al., 1996, 1999, 2001).

Table 2
a. Activations in Exp. 2 during the observation of the Arm, Arrow, and Colored Arm *vs.* each respective control still images; b. global activations during the observation of reaching movements independently of the stimulus-type. Local maxima of activated areas, as shown in Fig. 5, are given in MNI standard brain coordinates at cluster-level 0.05 and voxel level *P<.001 [ATB: most probable anatomical region in the Anatomy Toolbox 1.7, Eickhoff et al., 2005; asterisks (*) denote assigned areas].*

Anatomical region	Left					Right				
	x	*y*	*z*	*Z*-score	ATB	*x*	*y*	*z*	*Z*-score	ATB
a. Stim-type vs. control still image ($P_{UNCOR-VXL}$=<.001)										
Arm (Arm)										
Superior occipital gyrus/	−16	−98	20	7.17	60% Area 18*					
V6	−20	−82	28	4.35						
Middle occipital gyrus/V5	−42	−72	8	7.59	40% hOC5 (V5)*	48	−70	2	7.50	20% hOC5 (V5)*
Middle temporal gyrus/	−56	−68	12	4.30	20% IPC (PGp)					
STS	−48	−52	8	3.89						
Superior parietal lobule (SPL)	−32	−50	68	5.76	30% SPL (7PC)					
Precentral gyrus (PMd)	−28	−14	56	4.74	60% Area 6					
SMA	−8	14	48	4.45	20% Area 6	8	12	54	4.31	40% Area 6
Middle cingulate cortex						12	20	42	5.37	10% Area 6
Inferior frontal gyrus						48	18	4	4.21	20% Area 45
Superior frontal gyrus (medial)						6	28	46	3.93	10% Area 6
Middle frontal gyrus						38	46	20	4.39	
Insula	−36	20	−6	4.18		32	24	12	3.92	
Putamen	−28	24	−2	4.53						
Arrow (A)										
Superior occipital gyrus/	−16	−100	20	7.32	20% Area 18					
V6	−20	−82	24	3.53						
Middle occipital gyrus/V5	−44	−76	6	6.70	50% hOC5 (V5)*					
Superior parietal lobule	−32	−50	68	5.73	30% SPL (7PC)					
Inferior parietal lobule	−38	−38	38	4.66	30% hIP3*					
SupraMarginal Gyrus (TPJ)	−46	−40	30	4.50	40% IPC*					
precentral gyrus (PMd)	−36	−2	52	5.06	30% Area 6	36	−4	46	4.17	40% Area 6
SMA	−6	2	54	4.69	80% Area 6	6	16	50	3.91	40% Area 6
Middle cingulate cortex						10	20	42	5.03	10% Area 6
Superior medial gyrus						6	28	48	3.31	10% Area 6
Insula	−30	24	−2	4.88		32	22	−2	4.66	
Cerebellum	−20	−64	−30	4.43	81% Lobule VI (Hem)*					
Colored arm (CArm)										
Superior occipital gyrus/	−18	−92	24	6.66	10% Area 18					
V6	−20	−82	28	4.34						
Middle occipital gyrus/V5	−44	−74	8	7.49	20% hOC5 (V5)*					
Middle temporal gyrus/V5						46	−68	4	6.34	40% hOC5(V5)*
Superior parietal lobule	−30	−50	70	6.60	20% SPL (7PC)					
Precentral gyrus (PMd)	−34	−2	54	4.62	20% Area 6					
SMA	−6	4	52	4.92	70% Area 6	8	18	50	3.62	20% Area 6
Middle cingulate cortex						10	20	42	3.92	10% Area 6
b. Global analysis vs. control still image ($P_{COR-VXL}$=<.05)										
Arm+A+CArm										
Superior occipital gyrus/	−16	−94	34	Inf	10% Area 17					
V6	−20	−82	24	7.04						
Middle occipital gyrus/V5	−44	−76	6	Inf	50% hOC5(V5)*					
Middle temporal gyrus/V5						48	−68	2	Inf	30% hOC5(V5)
Superior parietal lobule	−32	−50	68	Inf		30	−56	68	6.10	40% SPL (7PC)*
SupraMarginal gyrus (TPJ)	−48	−38	32	Inf	30% IPC (PFcm)					
Inferior parietal lobule	−42	−32	40	5.35	40% IPC (PFt)*					
Precentral gyrus (PMd)	−34	−2	54	Inf	20% Area 6	40	−2	54	6.74	40% Area 6
SMA	−4	4	56	7.50	70% Area 6	8	18	50	6.72	20% Area 6
Middle cingulate cortex						10	20	42	7.05	10% Area 6
Inferior frontal gyrus						34	30	10	5.04	
Middle frontal gyrus	−36	48	20	5.68		36	44	16	7.20	
Insula	−30	20	2			28	20	−4	5.85	

Neuroanatomical data in the monkey further suggest that the dorsal sector of V6A (V6Ad; Luppino et al., 2005; Gamberini et al., 2011) receives information also from the inferior parietal lobule (IPL) and, more specifically, from area PG, which, in turn, receives input from the STS region (Rozzi et al., 2005, 2008) in response to complex biological movements (Grossman and Blake, 2001; Perrett, 1999; Thompson et al., 2005). It is therefore possible that the activation of SPL to movement velocity of the biological shape could be also due to its connections with V6 complex and related areas (STS, PG).

As far as the activation of dorsal premotor cortex is concerned, the neural substrate for its activation should include again the V6 complex that sends input directly to dorsal premotor cortex, as well as to other connected areas. In the monkey, in fact, connections have been suggested between V6 and F2 (Gamberini et al., 2009), and with MIP as well as between SPL (PEc) and F2 (Matelli and Luppino, 2001).

As a final point, some observations should be made with respect to the RS effects observed in this study. In fact, some authors have appropriately recommended that caution should be exercised in the interpretation of RS effects on brain activations (see Bartels et al., 2008; Tolias et al., 2005). Nonetheless, the results of the present study show that *f*MRI is capable to highlight functionally relevant processes in response to specific stimulus properties. In particular, the RS results of this study revealed activity enhancement in dorsal premotor and superior parietal cortex in response to velocity only for the biological effector, namely the arm, and not for the arrow that underwent the same RS procedure as the arm. Additionally, concerns with respect to the RS technique

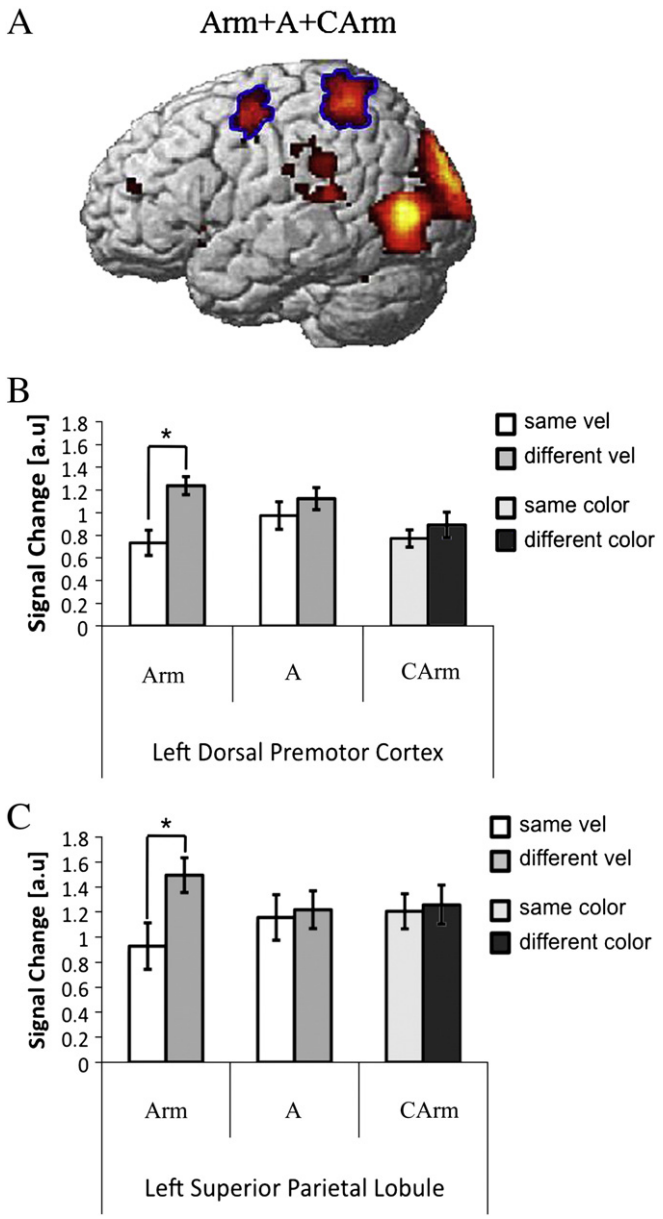

Fig. 6. Anatomical locations (A) projected on a standard MNI brain template of the region of interest (ROIs) built within the left dorsal premotor (PMd; maxima: −34 −2 54) and left superior parietal lobule (SPL; −32 −50 68) on the basis of the functional maps obtained from the global analysis among the three stimulus-types (Arm, A, CArm) in Exp. 2. The graphs display signal change produced by the conditions *same* and *different* for each stimulus-type (Arm, arrow — A, colored arm — CArm) within each ROI (B, PMd; C, SPL). The error bars represent the standard error of the mean. Asterisk (*) indicates significant differences between the conditions *different* — *same* Bonferroni corrected ($P \leq .017$). (For interpretation of the references to color in this figure legend, the reader is referred to the web version of this article.)

have been put forward suggesting that attention-related factors may affect brain activation when viewing two consecutive stimuli that differ from one another (Bartels et al., 2008). To control for attention-related confounds, we introduced, alongside the arm and the arrow stimuli, videos showing a reaching colored arm changing color, instead of velocity, in the conditions *different*. The lack of RS effect in the parietal and frontal sites for the colored arm allows us to further rule out the possibility that attention-related factors affected the RS results observed for the arm movement velocity.

In conclusion, in line with the more general mirror mechanism hypothesis, the results obtained in the present study suggest that the joint activation of SPL and PMd could represent the neural substrate underpinning the processing of reaching movement performed by others. The processing of reaching velocity of the biological shape could represent a functional property of these sites that enables one to understand *how* an action is performed when observing another individual.

Table 3
Descriptive analyses and the statistical values in Exp. 2 relative to the direct comparison between conditions *same* and *different* for each stimulus-type (Arm, A, CArm) in left PMd and SPL ROIs.

Location	Maxima	Condition	Mean	SEM	*F*-test (*P*)	Part-η^2
Left SPL	(−30 −56 68)	Arm same	0.92	0.37	0.005*	0.44
		Arm diff	1.49	0.36		
		A same	1.15	0.28	0.65	0.01
		A diff	1.21	0.27		
		CArm same	1.20	0.30	0.71	0.01
		CArm diff	1.25	0.31		
Left PMd	(−34 −2 54)	Arm same	0.73	0.22	0.000*	0.69
		Arm diff	1.23	0.24		
		A same	0.97	0.15	0.28	0.08
		A diff	1.12	0.15		
		CArm same	0.77	0.19	0.36	0.05
		CArm diff	0.89	0.22		

* significant corrected (Bonferroni correction for per multiple comparisons $P \leq .017$).

Acknowledgments

We would like to thank Valerie Adams, Anna Anderson, and Bill Bimson (Liverpool; Expt. 1), as well as F. Fasano, G. Burani, G. Mantelli, M. Rinaldi and Doc. G. Crisi (Parma; Exp. 2) for their kind technical and administrative support. Additionally, we would like to thank D. Eaves (Teesside and Lancaster University), who kindly helped in checking the revised manuscript. Exp. 1 was partially funded by a research project grant from the Leverhulme Trust (F/00 185/K) to S. Vogt and N. Roberts. We are further grateful to Fondazione Cassa di Risparmio di Parma (CARIPARMA) for providing the infrastructure that made this work possible, and to the Agenzia Spaziale Italiana (ASI) which funded this project.

References

Bartels, A., Logothesis, N.K., Moutoussis, K., 2008. fMRI and its interpretations: an illustrations on directional selectivity in area V5/MT. Trends Neurosci. 9, 444–453.
Binkofski, F., Buccino, G., Posse, S., Seitz, R., Rizzolatti, G., Freund, H., 1999. A fronto-parietal circuit for object manipulation in man: evidence from an fMRI-study. Eur. J. Neurosci. 11 (9), 3276–3286.
Buccino, G., Binkofski, F., Fink, G.R., Fadiga, L., Fogassi, L., Gallese, V., Seitz, R.J., Zilles, K., Rizzolatti, G., Freund, H.J., 2001. Action observation activates premotor and parietal areas in a somatotopic manner: an fMRI study. Eur. J. Neurosci. 13, 400–404.
Buccino, G., Lui, F., Canessa, N., Patteri, I., Lagravinese, G., Benuzzi, F., Porro, C.A., Rizzolatti, G., 2004a. Neural circuits involved in the recognition of actions performed by nonconspecifics: an fMRI study. J. Cogn. Neurosci. 16, 114–126.
Buccino, G., Vogt, S., Ritzl, A., Fink, G.R., Zilles, K., Freund, H.J., Rizzolatti, G., 2004b. Neural circuits underlying imitation learning of hand actions: an event-related fMRI study. Neuron 42, 323–334.
Casile, A., Dayan, E., Caggiano, V., Hendler, T., Giese, M., 2009. Neuronal encoding of human kinematic invariants during action observation. Cereb. Cortex 20, 1647–1655.
Colby, C., Gattass, R., Olson, C., Gross, C., 1988. Topographical organization of cortical afferents to extrastriate visual area PO in the macaque: a dual tracer study. J. Comp. Neurol. 269, 392–413.
Culham, J., 2004. Human brain imaging reveals a parietal area specialized for grasping. In: Kanwisher, N., Duncan, J. (Eds.), Functional Neuroimaging of Visual Cognition: Attention and Performance. Oxford University Press, Oxford, pp. 417–438. Edition.
Dayan, E., Casile, A., Levit-Binnun, N., Giese, M.A., Hendler, T., Flash, T., 2007. Neural representations of kinematic laws of motion: evidence for action–perception coupling. PNAS 104 (51), 20582–20587.
Dè Sperati, C., Viviani, P., 1997. The relationship between curvature and velocity in two-dimensional smooth pursuit eye movements. J. Neurosci. 17, 1244–1259.
Decety, J., 1996. Neural representation for action. Rev. Neurosci. 7, 285–297.
di Pellegrino, G., Wise, S.P., 1991. A neurophysiological comparison of three distinct regions of the primate frontal lobe. Brain 114, 951–978.
Eickhoff, S.B., Stephan, K.E., Mohlberg, H., Grefkes, C., Fink, G.R., Amunts, K., Zilles, K., 2005. A new SPM toolbox for combining probabilistic cytoarchitectonic maps and functional imaging data. Neuroimage 25, 1325–1335.

Engel, S., Furmanski, C., 2001. Selective adaptation to color contrast in human primary visual cortex. J. Neurosci. 21, 3949–3954.
Fang, S., Murray, D., Kersten, S., 2005. Orientation — tuned fMRI adaptation in human visual cortex. J. Neurophysiol. 94, 4188–4195.
Filimon, F., Nelson, J., Hagler, D., Sereno, M., 2007. Human cortical representations for reaching: mirror neurons for execution, observation, and imagery. NeuroImage 37, 1315–1328.
Fogassi, L., Ferrari, P., Gesierich, B., Rozzi, S., Chersi, F., Rizzolatti, G., 2005. Parietal lobe: from action organization to intention understanding. Science 308, 662–666.
Friston, K.J., Holmes, A.P., Worsley, K.J., 1999. How many subjects constitute a study? Neuroimage 10, 1–5.
Friston, K.J., Glaser, D.E., Henson, R.N., Kiebel, S., Phillips, C., Ashburner, J., 2002. Classical and Bayesian inference in neuroimaging: applications. Neuroimage 16, 484–512.
Galletti, C., Fattori, P., Battaglini, P.P., Shipp, S., Zeki, S., 1996. Functional demarcation of a border between areas V6 and V6A in the superior parietal gyrus of the macaque monkey. Eur. J. Neurosci. 8, 30–52.
Galletti, C., Fattori, P., Kutz, D.F., Gamberini, M., 1999. Brain location and visual topography of cortical area V6A in the macaque monkey. Eur. J. Neurosci. 11, 575–582.
Galletti, C., Gamberini, M., Kutz, D.F., Fattori, P., Luppino, G., Matelli, M., 2001. The cortical connections of area V6: an occipito-parietal network processing visual information. Eur. J. Neurosci. 13, 1572–1588.
Gamberini, M., Passarelli, L., Fattori, P., Zucchelli, M., Bakola, S., Luppino, G., Galletti, C., 2009. Cortical connections of the visuomotor parietooccipital area V6Ad of the Macaque monkey. J. Comp. Neurol. 513, 622–642.
Gamberini, M., Galletti, C., Bosco, A., Breveglieri, R., Fattori, P., 2011. Is the medial posterior area V6a a single functional area? J. Neurosci. 13, 5145–5157.
Gibson, J., 1986. The Ecological Approach to Perception. Lawrence Erlbaum Associates, Hillsdale.
Grafton, S.T., Arbib, M.A., Fadiga, L., Rizzolatti, G., 1996a. Localization of grasp representations in humans by PET: observation compared with imagination. Exp. Brain Res. 112, 103–111.
Grafton, S.T., Arbib, M.A., Fadiga, L., Rizzolatti, G., 1996b. Functional anatomy of pointing and grasping in human. Cereb. Cortex 6 (2), 226–237.
Grèzes, J., Armony, J.L., Rowe, J., Passingham, R.E., 2003. Activations related to "mirror" and "canonical" neurons in the human brain: an fMRI study. NeuroImage 18, 928–937.
Grill-Spector, K., Malach, R., 2001. fMR-adaptation: a tool for studying the functional properties of human cortical neurons. Acta Psychol. (Amst) 107, 293–321.
Grill-Spector, K., Kushnir, T., Edelman, S., Avidan, G., Itzchak, Y., Malach, R., 1999. Differential processing of objects under various viewing conditions in the human lateral occipital complex. Neuron 24, 187–203.
Grossman, E.D., Blake, R., 2001. Brain activity evoked by inverted and imagined biological motion. Vis. Res. 41, 1475–1482.
Hamilton, A.F., Grafton, S.T., 2009. Repetition suppression for performed hand gestures revealed by fMRI. Hum. Brain Mapp. 30 (9), 2898–2906.
Hicheur, H., Vieilledent, S., Richardson, M.J.E., Flash, T., Berthoz, A., 2005. Velocity and curvature in human locomotion along complex curved paths: a comparison with hand movements. Exp. Brain Res. 162 (2), 145–154.
Huk, A.C., Ress, D., Heeger, D.J., 2001. Neuronal basis of the motion aftereffect reconsidered. Neuron 32, 161–172.
Iacoboni, M., Woods, R.P., Brass, M., Bekkering, H., Mazziotta, J.C., Rizzolatti, G., 1999. Cortical mechanisms of human imitation. Science 286, 2526–2528.
Jastorff, J., Begliomini, C., Fabbri Destro, M., Rizzolatti, G., Orban, G.A., 2010. Coding observed motor acts: different organizational principles in the parietal and premotor cortex of humans. J. Neurophysiol. 104 (1), 128–140.
Kourtzi, Z., Grill-Spector, K., 2005. fMRI adaptation: a tool for studying visual representations in the primate brain. In: Rodhes, G., Clifford, C.W.G. (Eds.), Fitting the mind into the World. Adaptation and after-effects in high-level vision. Oxford University Press, USA, pp. 173–188.
Laquaniti, F., Terzuolo, C., Viviani, P., 1983. The law relating the kinematic and figural aspects of drawing movements. Acta Psychol (Amst) 54 (1–3), 115–130.
Lestou, V., Pollick, F., Kourtzi, Z., 2008. Neural substrates for action understanding at different description levels in the human brain. J. Cogn. Neurosci. 20, 324–341.
Luppino, G., Hamed, S.B., Gamberini, M., Matelli, M., Galletti, C., 2005. Occipital (V6) and parietal (V6A) areas in the anterior wall of the parieto-occipital sulcus of the macaque: a cytoarchitectonic study. Eur. J. Neurosci. 21, 3056–3076.
Matelli, M., Luppino, G., 2001. Parietofrontal circuits for action and space perception in the macaque monkey. NeuroImage 14, 27–32.
Perrett, J.L., 1999. Constitution by movement: Husserl in light of recent neurobiological findings. In: Pettitot, J., Varela, F.J., Pachoud, B., Roy, J.M. (Eds.), Contemporary Phenomenology and Cognitive Science, Naturalizing Phonomenology. Stanford University Press, Stanford, pp. 220–224. Edition.
Pitzalis, S., Sereno, M., Committeri, G., Fattori, P., Galati, G., Patria, F., Galletti, C., 2009. Human V6: the medial motion area. Cereb. Cortex 20 (2), 411–424.
Rizzolatti, G., 2005. The mirror neuron system and its function in humans. Anat. Embryol. 210, 419–421.
Rizzolatti, G., Craighero, L., 2004. The mirror–neuron system. Annu. Rev. Neurosci. 27, 169–192.
Rizzolatti, G., Sinigallia, C., 2010. The functional role of the parieto-frontal mirror circuit: interpretations and misinterpretations. Nat. Rev. Neurosci. 11, 264–274.
Rizzolatti, G., Fadiga, L., Fogassi, L., Gallese, V., 1996a. Premotor cortex and the recognition of motor actions. Cogn. Brain Res. 3, 131–141.
Rizzolatti, G., Fadiga, L., Matelli, M., Bettinardi, V., Paulesu, E., Perani, D., Fazio, F., 1996b. Localization of grasp representation in humans by PET: observation versus execution. Exp. Brain Res. 111, 246–252.
Rizzolatti, G., Fogassi, L., Gallese, V., 2001. Neurophysiological mechanisms underlying the understanding and imitation of action. Nat. Rev. Neurosci. 2, 661–670.
Rozzi, S., Calzavara, R., Belmalih, A., Borra, E., Gregoriou, G.G., Matelli, M., Luppino, G., 2005. Cortical connections of the inferior parietal cortical convexity of the macaque monkey. Cereb. Cortex 16, 1389–1417.
Rozzi, S., Ferrari, P.F., Bonini, L., Rizzolatti, G., Fogassi, L., 2008. Functional organization of inferior parietal lobule convexity in the macaque monkey: electrophysiological characterization of motor, sensory and mirror responses and their correlation with cytoarchitectonic areas. Eur. J. Neurosci. 28, 1569–1588.
Sunaert, S., Van Hecke, P., Marchal, G., Orban, G., 1999. Motion-responsive regions of the human brain. Exp. Brain Res. 127, 355–370.
Thompson, J.C., Clarke, M., Stewart, T., Puce, A., 2005. Configural processing of biological movement in human superior temporal sulcus. J. Neurosci. 25, 9059–9066.
Tolias, A.S., Smirnakis, S., Augath, M., Trinath, T., Logothetis, N.K., 2001. Motion processing in the macaque: revisited with functional magnetic resonance imaging. J. Neurosci. 21 (21), 8594–8601.
Tolias, A.S., Keliris, G.A., Stelios, M.S., Smirnakis, S.M., Logothetis, N.K., 2005. Neurons in macaque area V4 acquire directional tuning after adaptation to motion stimuli. Nat. Neurosci. 8 (5), 591–593.
Viviani, P., Flash, T., 1995. Minimum-jerk, two third power law, and isochrony: converging approaches to movement planning. J. Exp. Psychol. Hum. Percept. Perform. 21, 32–53.
Viviani, P., Stucchi, N., 1992. Biological movements look uniform: evidence of motor-perceptual interactions. J. Exp. Psychol. 18 (3), 603–623.
Zeki, S., Watson, J.D.G., Lueck, C.J., Friston, K.J., Kennard, C., Frackowiak, R.S., 1991. A direct demonstration of functional specialization in human visual cortex. J. Neurosci. 11, 641–649.